Carbon dioxide migration along faults at the Illinois Basin – Decatur Project revealed using time shift analysis of seismic monitoring data

Idris Bukar[1*], Rebecca Bell[1], Ann Muggeridge[1], Samuel Krevor[1]

[1*]Department of Earth Science and Engineering, Imperial College London, Royal School of Mines, London, SW7 2BP, United Kingdom.

*Corresponding author(s). E-mail(s): i.bukar21@imperial.ac.uk; Contributing authors: rebecca.bell@imperial.ac.uk; a.muggeridge@imperial.ac.uk; s.krevor@imperial.ac.uk;

Abstract

Large scale underground storage of CO_2 is being deployed worldwide to reduce greenhouse gas emissions to the atmosphere. Modelling studies have investigated the possible risks from the CO_2 migrating along faults, but this has not yet been observed. We were able to identify such CO_2 migration at a commercial-scale, demonstration CO_2 storage project, the Illinois Basin - Decatur Project, including subsequent emergence of the CO_2 into overlying permeable layers. Our interpretation resolves previous inconsistencies observed at the project and provides a rare field observation the fluid dynamics of CO_2 moving between faults and reservoir lithology. The project had deployed time-lapse 3D vertical seismic profile imaging to study CO_2 plume development, interpreted based on the commonly used amplitude attributes. However, factors including survey repeatability, subtle seismic fluid effects and irregular filling of the storage reservoir by CO_2 meant that amplitude anomalies due to CO_2 were not distinct. Here we apply an alternative interpretation technique to the data based on time shift attributes, resulting in much clearer plume anomalies. This work provides field validations of previously theorised plume behaviours and demonstrates the use of an alternative analysis technique to overcome challenges in interpretation of seismic monitoring data for geological CO_2 storage.

Introduction

Carbon capture and geological storage is being scaled up worldwide to achieve net zero carbon emissions by 2050 (Krevor et al., 2023; Pörtner et al., 2022). Monitoring CO_2 storage through time-lapse seismic techniques has provided observations of the flow and trapping behaviour of the injected CO_2 at storage projects around the world (Furre et al., 2017; Hansen et al., 2013; Ivandic et al., 2015; Roach & White, 2018). The observations have revealed fluid dynamics which are more complex and dynamic than analogous subsurface fluids systems due to the properties of CO_2 as a supercritical fluid at reservoir conditions (Cavanagh & Haszeldine, 2014; Ringrose et al., 2022).

Of particular interest is the potential for CO_2 to move buoyantly upwards from a target reservoir through leakage pathways such as a fault or wellbore, and this has been investigated using geological analogues, and theoretical and numerical modelling (Gasda et al., 2004; Gilmore et al., 2022; Miocic et al., 2016; Nordbotten et al., 2009). There are no instances of CO_2 leakage from currently operating storage projects. However, CO_2 escape from natural subsurface accumulations is observed primarily through faults, and the escape of hydrocarbon gases through wellbores is pervasive (Dockrill & Shipton, 2010; Faulkner et al., 2010; Jung et al., 2014; Kang et al., 2016; Miocic et al., 2016; Onishi et al., 2019). Models of these systems show that complex dynamics emerge depending on the permeabilities of fault zones relative to reservoir units, and CO_2 migration up leakage pathways can in some instances be entirely mitigated by trapping as the plume emerges in overlying permeable strata. Despite their importance, the hydraulic properties of fault zones are notoriously difficult to evaluate, and there are no engineered settings in which the movement of CO_2 along faults has been observed.

However, while time-lapse seismic surveys provide a means for observation of fluid movement over time, their acquisition and processing must be performed in a way that maximises repeatability (Johnston, 2013). In general, land seismic surveys can suffer from significantly more noise than marine seismic surveys due to scattering by the near surface layer (Stork, 2020). Time-lapse 3D (i.e. 4D) vertical seismic profile (VSP) surveys at the onshore Illinois Basin – Decatur Project CO_2 storage site, the focus of this work, were affected by seasonal variations in ground conditions and source co-location issues due to infrastructure development and permitting difficulties (Couëslan et al., 2013). The project used an interpretation approach for the 4D data that is based on amplitude difference (Couëslan et al., 2014) and normalised RMS amplitude difference attributes (Bauer et al., 2019). The results were ambiguous due to weak time-lapse signals (Couëslan et al., 2013). During the post-injection phase, the project detected an isolated finger of CO_2 in the injection well in a shallower zone than the injection interval (Zaluski & Lee, 2021), and the lack of seismic monitoring during that period meant the origins of the CO_2 could not be ascertained.

We used time shift attributes to analyse the seismic monitoring data at Decatur, a technique that has been applied successfully to monitor fluid movement in oil and gas reservoirs (Benguigui et al., 2012; Falahat et al., 2011; Santos et al., 2016) and to support amplitude interpretation at CO_2 storage sites (Arts et al., 2004; Chadwick et al., 2004, 2005; Furre et al., 2015; Grude et al., 2013). The results resolve inconsistencies in the previous interpretation, revealing that the CO_2 plume at Decatur has been migrating along major faults previously characterised in the reservoir, and moving in response to injection at a neighbouring site. The analysis thus provides an important dataset of previously theorised plume migration behaviour between fault zones and reservoir units, while demonstrating the superiority of a seldom used approach to time-lapse seismic analysis.

Results and Discussion

Interpretations of CO_2 plume anomalies from seismic monitoring data

We interpret CO_2 plumes qualitatively from the results of time shift analysis, identifying several plume layers, with the largest layer in the injection interval (the lower unit of the Mt. Simon A formation). A second plume layer is identified in the upper unit of the Mt. Simon A formation, and a third and fourth layer in the Mt. Simon C formation. Figure 1 (a) shows a map view of three layers located at different depths as interpreted from the first time-lapse monitor. Figures 1 (b) and (c) show cross sectional views of the plume layers. Also shown are three out of 28 faults interpreted to transect parts of the Mt. Simon formation. These faults were interpreted prior to injection, from 3D seismic data acquired during site characterisation. Most of the faults have small displacements relative to the thickness of the Mt. Simon, with the largest vertical displacement estimated to be about 18 m. All interpreted plume anomalies exceed the lateral coverage of the seismic monitoring cubes. This is because the VSP surveys employed have a limited imaging aperture given that the receiver array is located in a well.

We check the plume results from our analysis against saturation measurements acquired in the wells. The seismic results show that layers 1 and 3 should be detected in injection well CCS1, but not layer 2 which does not reach the well. Observations from the repeat saturation logs confirm this expectation. However, while monitoring well VW1 shows a detection of an approximately 2 m

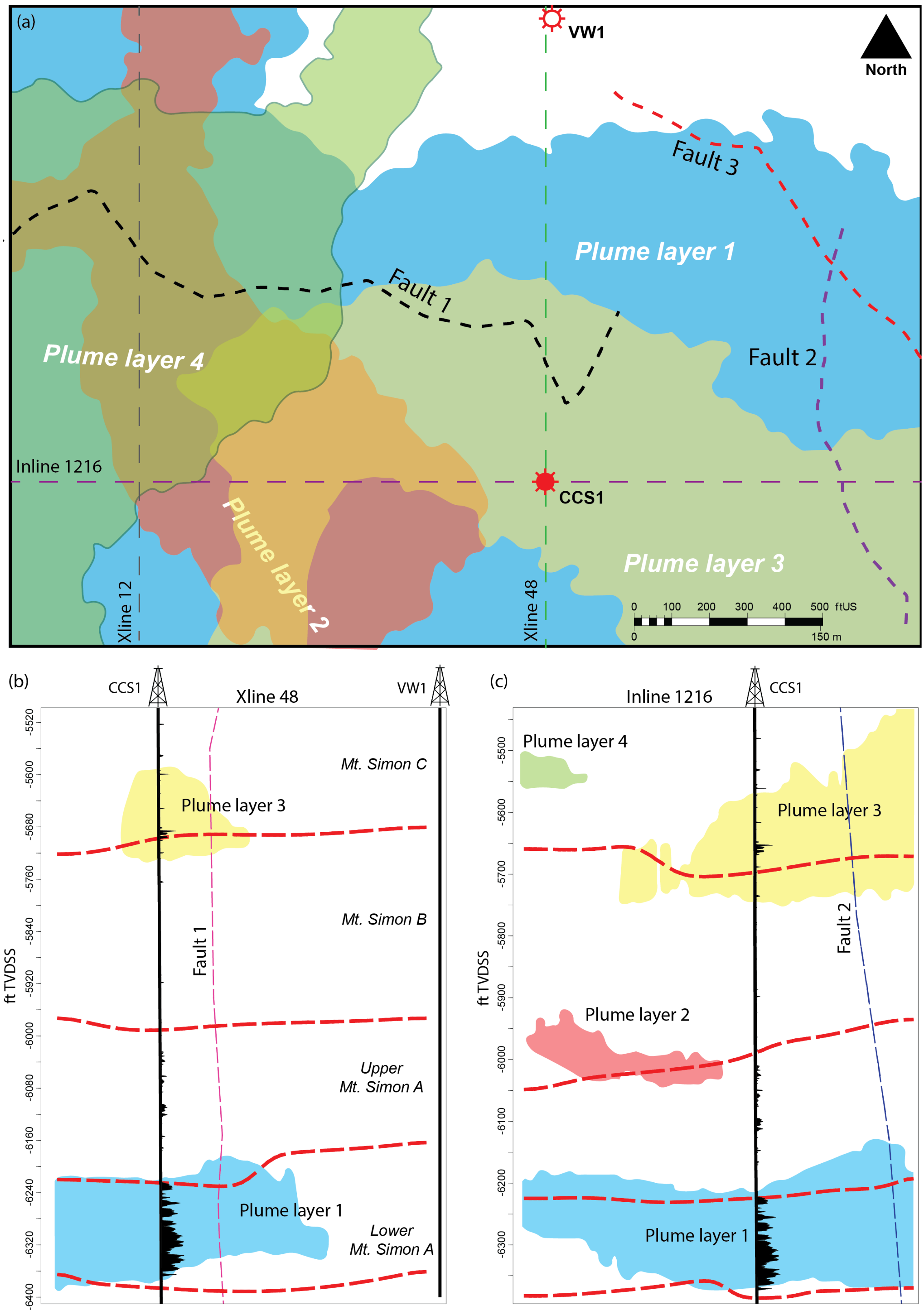

Fig. 1 (a) A map view of interpreted plume layers from time shift analysis at different depths for the first monitor. (b), (c) Cross sections along the inline and crossline marked in (a). CO_2 saturation from well logging measurements at a time corresponding to the first monitor is shown along the well path. Thicknesses of the upper plume layers appear exaggerated due to the low frequency characteristics of the seismic data.

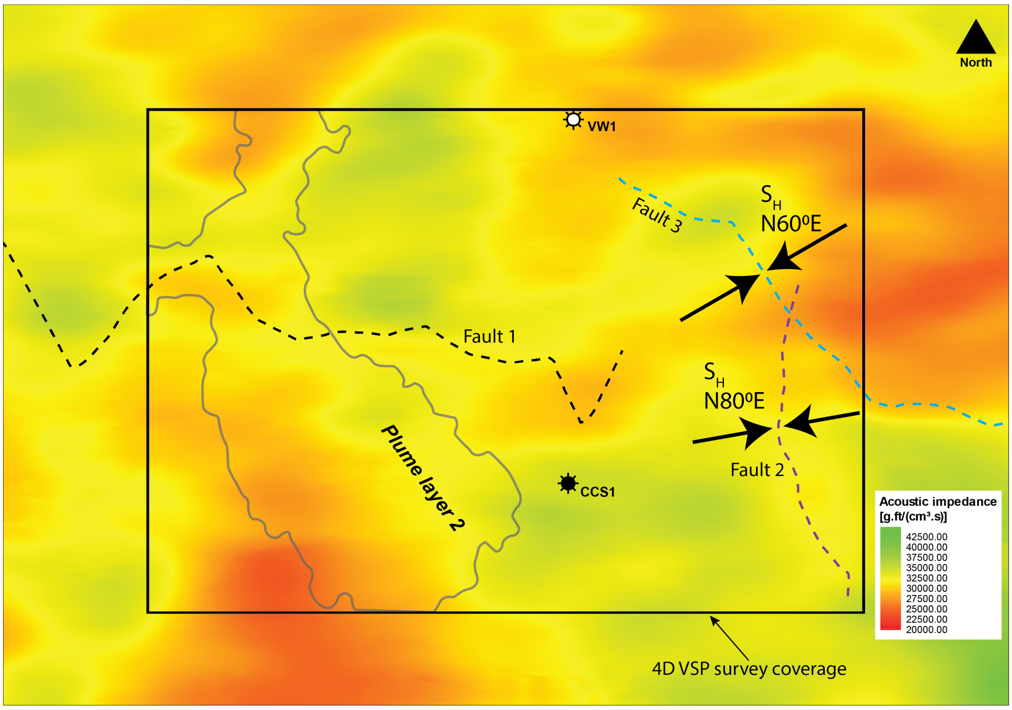

Fig. 2 Reservoir quality represented by acoustic impedance, with low values (red and yellow) corresponding to high quality regions. Slice shown is at 6000 ft TVDSS. CO_2 plume layer 2 interpreted from 4D VSP within the coverage at the corresponding depth appears to track high quality regions of the reservoir. Faults 2 and 3 have their planes oriented sub-perpendicular to the direction of maximum horizontal stress, S_H, which ranges between N60°E to N80°E, and are therefore sealed shut.

thick layer 1 from the saturation log, the interpreted CO_2 plume layer 1 from seismic does not reach the well. Given that the seismic wavelength at the depth of the injection interval is about 80-100 m, we do not expect a 2 m thick plume of low saturation to be detected. Moreover, in the third monitor, by which time 730,000 t of CO_2 had been injected and the gross thickness of the plume at VW1 from the saturation logs was about 18 m thick, it is detected from the seismic results (Figure S.3 in the Supplementary Information). The saturation logs show that the upper plume layers are thin (layer 3 is about 5 m at the location of well CCS1), however, their thicknesses from seismic appear exaggerated due to the low frequency characteristics of the data. The plume features from all monitors are qualitatively very similar as observed within the narrow monitoring cubes (Figure S.3 in the Supplementary Information). This suggests that the vertical distribution behaviour, including flow through faults, developed quite early, within four months of injection. Therefore, with increasing mass of injected CO_2 over time, we expect the major differences to be in the lateral footprint, which the narrow cubes make impossible to fully observe.

The irregular plume shapes produced by the shallower CO_2 layers appear to be controlled by reservoir quality. As shown in Figure 2, the outline of plume layer 2 tracks the high quality regions as the CO_2 avoids the poor quality areas. We use a 3D volume of acoustic impedance, a product of rock bulk density and P-wave velocity, to represent reservoir quality. Zones of high acoustic impedance represent low quality or tight zones and vice-versa. The acoustic impedance volume was derived from inversion of 3D seismic data acquired for site characterisation. Acoustic impedance is a good proxy for reservoir quality in this case because the primary cause of poor reservoir quality in the upper units of the Mt. Simon is Quartz cementation (Freiburg et al., 2014), which typically results in higher P-wave velocities by stiffening the rock frame. Cementation also means porosity destruction, which raises rock bulk densities.

Capillary and permeability barriers and vertical CO_2 containment

Early modelling attempts at the Decatur site evaluated the risk of extensive lateral migration as low and expected a more vertical filling of the lower Mt. Simon sandstone by the injected CO_2 (Finley et al., 2013). This informed the design of the time-lapse VSP surveys used for studying the plume development (Couëslan et al., 2009). From observation of the time-lapse saturation logs, it can be interpreted that contrary to those expectations, the injected CO_2 preferentially fills the high quality reservoir sandstones and avoids poorer quality or tight sandstones (Figure 3). We define tight sandstones as those with low porosity, low permeability and high capillary entry pressure. Strandli and Benson, 2013 and Strandli et al., 2014 show that there is excellent pressure communication between the two zones where the fingers of the plume are detected in VW1 (zones 2 and 3 in Figure 3), with both bottomhole pressure gauges showing identical behaviours and near-instantaneous responses to varying injection rates. Nonetheless, the lower finger does not at any point buoyantly rise and coalesce with the upper finger, even after injection had ceased, as it is held back by a tight zone at 6294 ft (Figure 3). The upper finger is also contained by another tight zone at 6251 ft. These tight zones clearly have sufficient permeability to allow good pressure communication across and even allow the flow of displaced brine as shown by Strandli et al., 2014. This suggests that these tight zones are capillary barriers rather than permeability barriers.

We however do not discount the presence of permeability barriers in the lower Mt. Simon. One such barrier is a mudstone layer of about 1.8 m thickness at 6182-6186 ft in VW1. Strandli et al., 2014 show that this layer restricts pressure propagation between zones 2 and 3 below it and zone 4 above it. However, this mudstone layer is discontinuous; it is missing in the injection well and is penetrated by only two out of the four wells at the site. These mudstones have been interpreted by Leetaru and Freiburg, 2014 to be interbedded within the Mt. Simon A formation but having a low

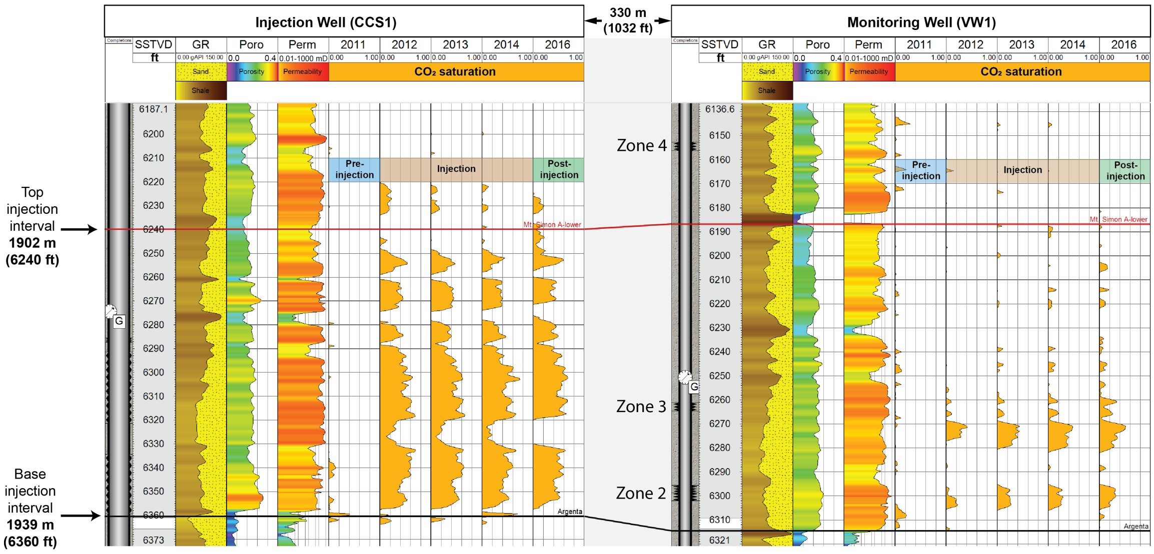

Fig. 3 Well log panels for the injection and monitoring wells showing reservoir properties and repeat saturation logging measurements from pre-injection, through the injection period to post-injection.

preservation potential in an ephemeral fluvial environment. This is evidenced by occasional mudstone clasts observed in core from well VW1, likely the eroded remnants of the original mudstone deposits (Leetaru & Freiburg, 2014). This is in addition to their complete absence in two wells. Therefore, the general vertical containment of CO_2 within the lower unit of the Mt. Simon A formation (the injection interval) cannot plausibly be attributed to them.

CO_2 migration along faults locally within the Mt. Simon and subsequent emergence

We interpret CO_2 flow along faults within the Mt. Simon, while it remains contained within high quality zones, all below the sealing primary caprock. As shown in Figure 4, the main plume of CO_2 in the injection interval is contained within the lower unit of Mt. Simon A. The acoustic impedance slice representing reservoir quality shows the lack of high quality pathways through the rock matrix for CO_2 to migrate upwards from the injection interval. Saturation logs in CCS1 confirm this as they show no continuous CO_2 saturation along the rest of the profile between the detections of layer 1 and layer 3 (Figure 3). The origin of the CO_2 detected in the overlying zones, therefore, requires an alternative explanation. We thus interpret that at least the east-west trending fault 1 shown in Figure 1 to be hydraulically conductive and transmitting CO_2 upwards along its apertures under gravity, and feeding the upper plume layers from layer 1. Buoyant CO_2 fluid contained within layer 1 preferentially channels upwards along the fault rather than through the overlying capillary barrier.

CO_2 entry into the fault implies a lower capillary entry pressure through the fault apertures. We propose that CO_2 flows through the fault and emerges when it reaches a point where the reservoir is of high quality, or a point beyond which the fault zone has lower permeability. This is illustrated in Figure 4.

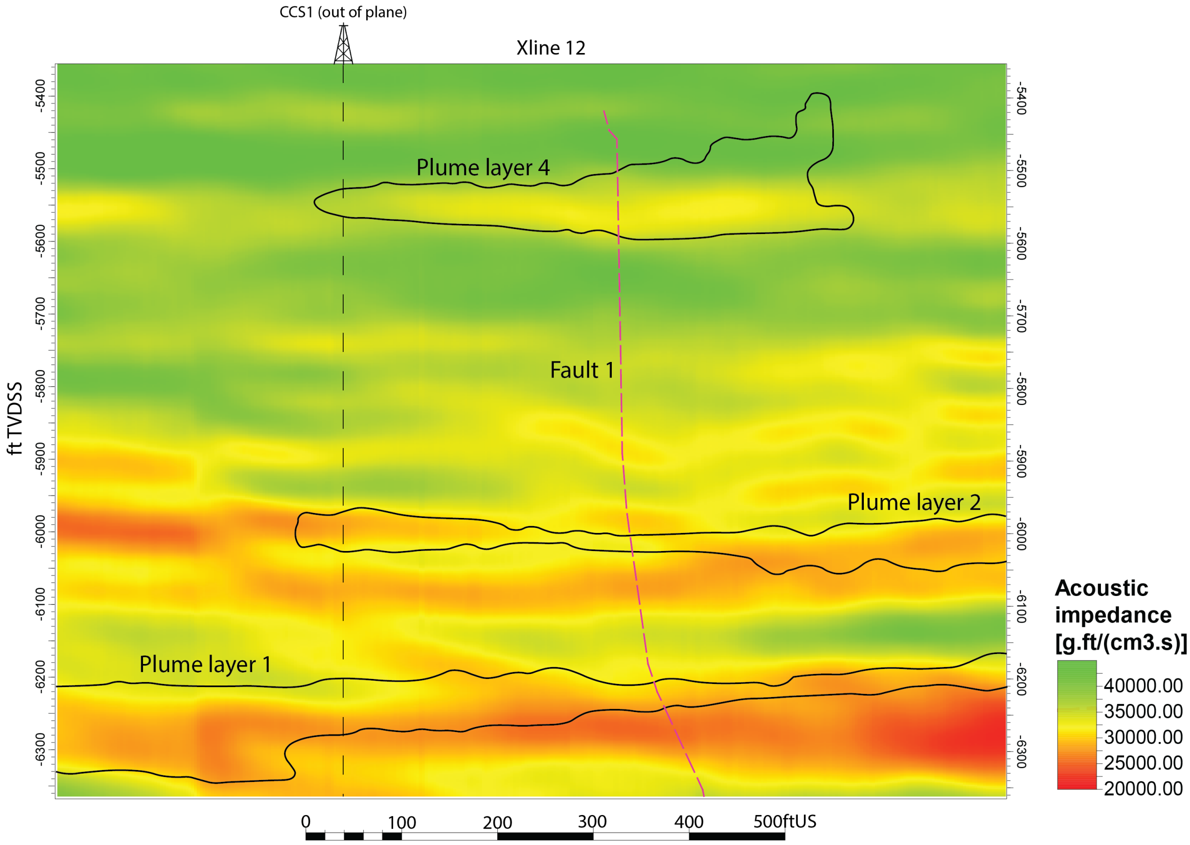

Fig. 4 Acoustic impedance from 3D seismic inversion used as a proxy for reservoir quality. Interpreted plume outlines are shown to be prevented from buoyantly rising by tight zones or capillary barriers (green regions) and instead channel through permeable faults.

We interpret fault 2 and fault 3 (Figure 2) to be non-conductive. This is because we do not detect the emergence of CO_2 around the faults in the high quality zone at the eastern flank of the monitored area. This could be because the faults are kept closed by compressive stresses. The Illinois Basin lies within the east-northeast to west-southwest compressive stress field of the eastern part of the North American plate, with the maximum horizontal stress orientation ranging between N60°E to N80°E (Lahann et al., 2017). This could provide a reasonable explanation as to the non-conductive nature of these faults, which are sub-perpendicular to the direction of maximum horizontal stress. The generally east-west trending fault 1, conversely, appears conductive and probably solely responsible for feeding the overlying plume layers. The behaviour of CO_2 emergence in a high quality zone could mitigate leakage up conductive faults as the amount of CO_2 that continues to migrate up a fault is progressively reduced with each encountered high quality zone. Where the conductive faults are intra-reservoir and do not traverse the seal, they would merely serve to provide access to other good quality zones of the reservoir, distributing the CO_2 among them, as has been shown through modelling (Yang et al., 2018; Zhang et al., 2024). Such is the case for the Decatur project; the fault provides flow pathways to overlying good quality zones of the Mt. Simon formation, which the injected CO_2 is unable to access normally due to capillary barriers.

Origins of late CO_2 arrival at injection well post-injection

An isolated finger of CO_2 was detected in the injection well during the post-injection period of the project in May 2018. This CO_2 was detected in the upper unit of the Mt. Simon A formation, and it increased in saturation in the March 2019 survey (Figure 5). The saturation logging report (Swager, 2019) suggested the origins of the CO_2 to be the Illinois Industrial Carbon Capture and Storage project located about 1100 m north of well CCS1. The injection well at this secondary project, well CCS2, had been injecting into the upper unit of the Mt. Simon A formation for 13 months at the time of detection.

A simplified mass and volume balance analysis shows it is unlikely that enough CO_2 had been injected in well CCS2 to have reached well CCS1 at the time of detection. We consider flow through only one-third the thickness of the injection zone at a conservative CO_2 saturation of 0.2 and with no dissolution. The resulting plume footprint equivalent to 687,000 t of CO_2 that had been injected at the time is shown in Figure 5 (a). In addition, the uppermost part of the A-Upper unit (c. 5950 ft in well CCS2) has the highest reservoir quality throughout the entire Mt. Simon sandstone, with permeabilities up to 1000 mD. Given the excellent correlation of this interval across the three wells, it is the most likely pathway for any rapid migration of CO_2. However, the late arriving CO_2 was detected instead in an interval in the lower half of the unit at a depth of 6150 ft. This interval is deeper than the injection zone in CCS2, which would require the CO_2 to flow downdip. This is unlikely outside the viscous region due to buoyancy forces. Moreover, no CO_2 was detected in the corresponding interval of well VW1, which is located between wells CCS2 and CCS1. This is summarised in Figure 5 (b).

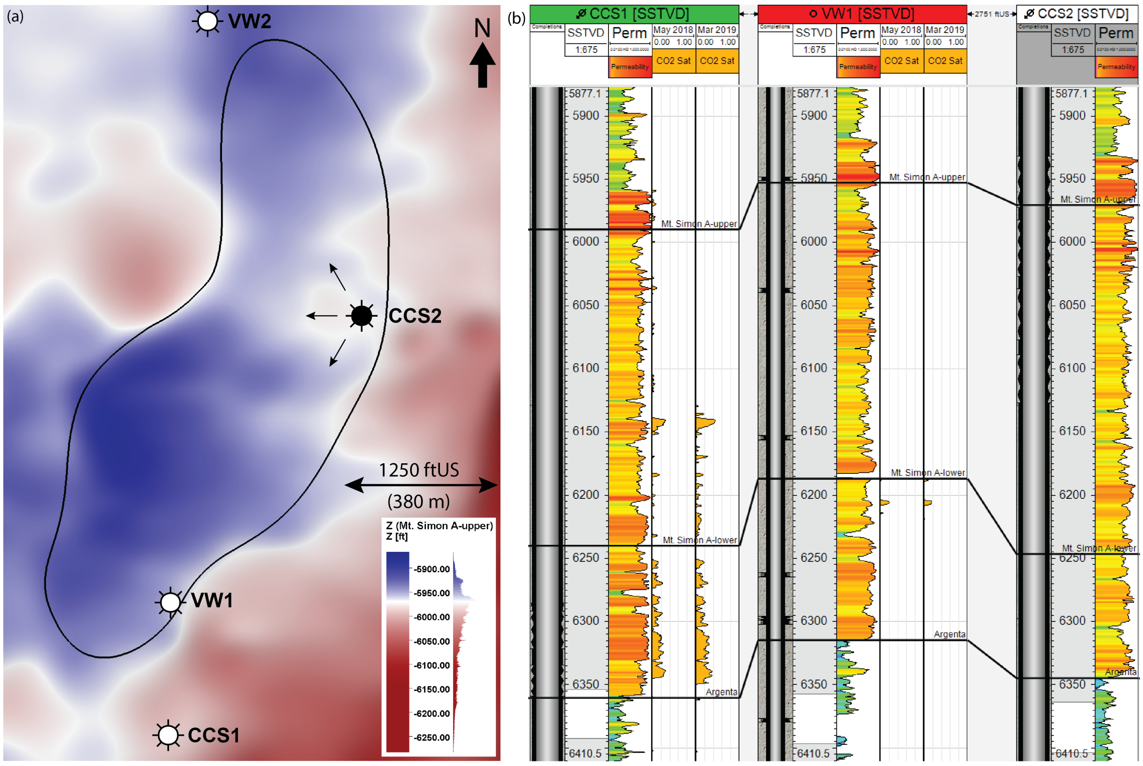

Fig. 5 (a) CO_2 plume footprint equivalent to 687,000 t of CO_2 derived using a simplified mass and volume balance. (b) Well correlation panel showing wells CCS1, CCS2 and VW1 with no CO_2 detection at VW1.

We present an alternative hypothesis based on plume interpretations from seismic time shift analysis and pressure and saturation logging data. We propose that the CO_2 instead originated from the CCS1 well – the same well it was detected in – but from layer 1 in the underlying injection interval. The evidence supports that the CO_2 travelled vertically through Fault 2, forming layer 2 as shown in Figure 1. Over time, layer 2 got larger as more CO_2 pooled. Once injection began at the nearby Illinois Industrial Carbon Capture and Storage project, the pressure gradient induced as a result of active CO_2 injection in well CCS2 then forces layer 2 to flow across the face of CCS1, resulting in this new detection. We argue this given that bottomhole pressure data shows good pressure communication between wells CCS1 and CCS2. Our interpretation of the overall CO_2 migration behaviour during the three stages of CCS1 injection, post CCS1 injection and CCS2 injection is summarised in Figure 6.

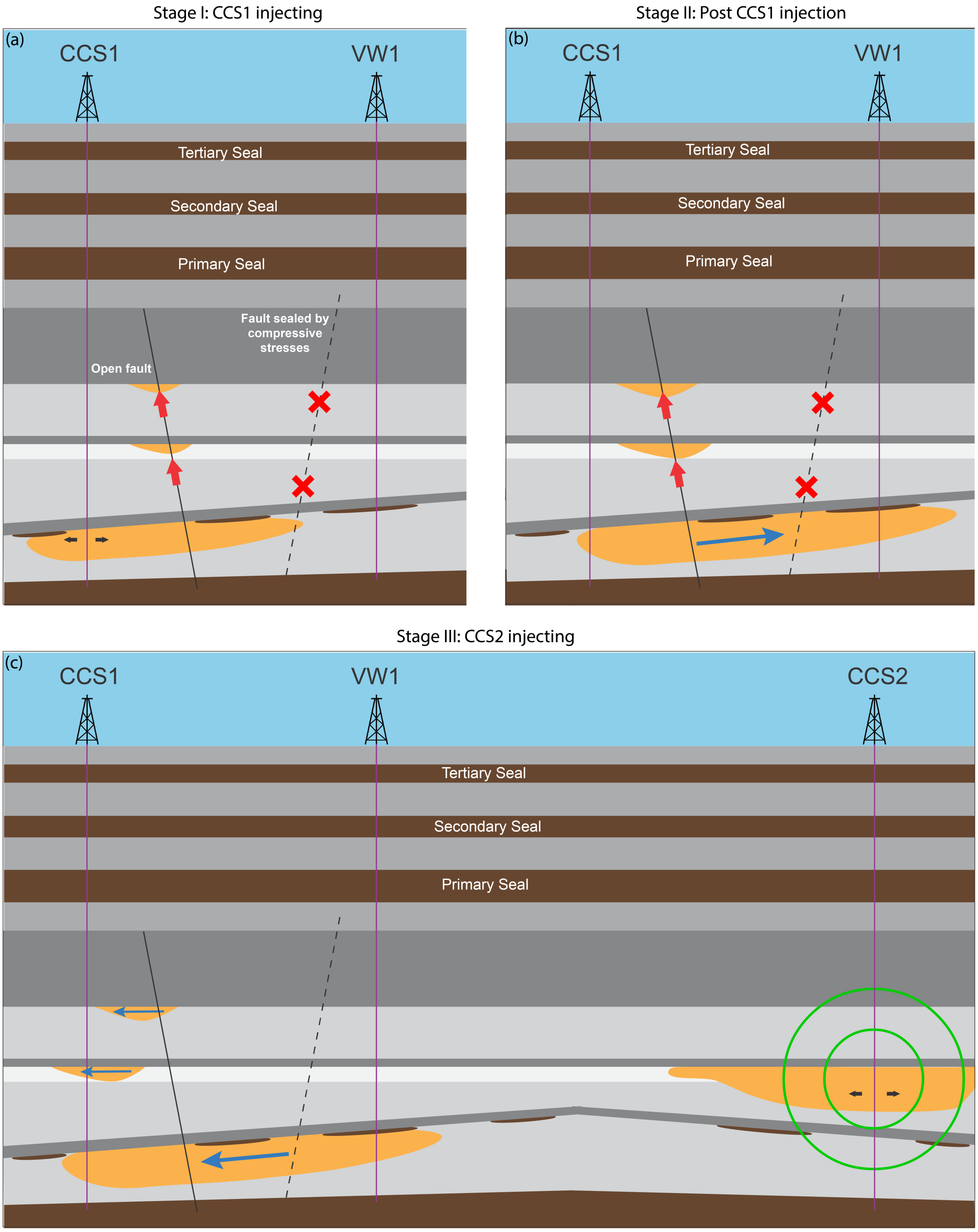

Fig. 6 A conceptual schematic summarising the overall plume behaviour during (a) CCS injection, (b) post CCS1 injection, and (c) CCS2 injection. Reservoir quality is indicated in grayscale with darker tones representing tight zones. Faults are classified as either open or sealed depending on the orientation of their planes with respect to the direction of maximum horizontal stress.

Conclusion

We have re-interpreted data from seismic surveys at the Illinois Decatur Basin Project and shown that the CO_2 plume has been migrating along major faults between high quality units of the reservoir, and moving laterally in response to injection at a neighbouring site. The analysis provides an important dataset of previously theorised plume migration behaviour between fault zones and reservoir units. This interpretation was otherwise not possible using a conventional analysis of amplitude attributes. Survey repeatability issues including source point co-location difficulties and changing ground conditions introduced spurious amplitude anomalies that subtle fluid-related amplitude anomalies were indistinguishable from. Furthermore, although the lower Mt. Simon reservoir is thick, the CO_2 plume does not fill it uniformly and instead forms thin layers that are not fully resolvable by the seismic data which therefore suffers from tuning of amplitudes. These factors may occur commonly in projects and are unfavourable to an amplitude-based interpretation, especially in onshore settings. The much clearer picture of CO_2 plume anomalies provided by time shifts enabled the overall analysis by allowing a meaningful integration of multiple independent measurements to produce a coherent interpretation of the migration behaviour of injected CO_2 at the Decatur site. We were able to identify an interplay of capillary heterogeneity and upward flow of CO_2 along permeable faults under buoyancy forces. In addition, we identify the role of pressure gradients resulting from CO_2 injection at a neighbouring project in causing the re-mobilisation and flow of CO_2 at the Decatur project post-injection. These behaviours and their impacts have been previously theorised and the observations provided from an industry scale geological CO_2 storage site provides important validation of these theories and data from which future projects may be designed.

Methods

Monitoring Data from the Illinois Basin - Decatur Project

The Illinois Basin - Decatur Project injected 1 Mt of CO_2 over three years from 2011 to 2014, into the Mt. Simon sandstone at a depth of c. 2100 m. The Mt. Simon sandstone is a Cambrian-age saline aquifer and is one of the major CO_2 sequestration resources in the United States. It is over 450 m thick at the Decatur site. Leetaru and Freiburg, 2014 and Freiburg et al., 2014 provide a detailed depositional and diagenetic characterisation of it at Decatur. It is unconformably overlain by the Eau Claire Formation, which is a predominantly shale formation over 90 m thick at the Decatur site and serves as the primary caprock for the storage unit. The Mt. Simon Sandstone is subdivided into upper, middle and lower formations. The best reservoir quality occurs in the lower Mt. Simon formation, with porosities of up to 28% and permeabilities of up to 1000 mD, and an average porosity and permeability of 22% and 200 mD. The lower unit of this formation is the injection interval for the project. The project has an injection well (CCS1) and a monitoring well (VW1). Wells CCS2, VW2 are the injection and monitoring wells for the nearby Illinois Industrial Carbon Capture and Storage project. The monitoring data and the data previously acquired for site characterisation form an excellent dataset for studying the complex behaviour of CO_2 plumes in the field. The dataset comprises in-well and geophysical monitoring data including time-lapse 3D VSP surveys. The in-well monitoring data includes bottomhole pressures, injection rates and repeat saturation logs. These logs recorded CO_2 saturation profiles periodically in wells CCS1 and VW1. They provide a time-lapse 1D profile of CO_2 saturation at the high resolution of wireline logging tools. Time-lapse 3D VSP surveying was chosen as the main geophysical monitoring technique to monitor the CO_2 plume in three dimensions. These surveys were meant to provide information on the plume development over time. They were acquired using surface seismic sources with receivers permanently installed in a shallow geophysical monitoring well GM1 located 60 m northwest of the injection well. Surveys were acquired each year from 2012 to 2015, with Baseline 2 being the reference pre-injection survey. Analysis of the time-lapse vertical seismic profile data is the main focus of this work. The survey dates, ground conditions during acquisition and injected CO_2 mass are reported by Couëslan et al., 2013.

Amplitude and time shift attributes

Previous investigations used amplitude attributes including normalised RMS (NRMS) and amplitude difference (Bauer et al., 2019; Couëslan et al., 2013). We reproduce those analyses by extracting both amplitude difference and NRMS. The attributes do not produce distinct CO_2 plume features as there is a pervasive presence of amplitude anomalies including above the primary seal and below the reservoir in the pre-Cambrian basement (Figure S.1 in the Supplementary Information). We perform an analysis of time shifts in an attempt to overcome these difficulties in interpretation. Time shifts provide a measure of changes in the two-way travel time of a seismic wave between two surveys, where an increase in travel time results from a slowdown of seismic waves by a lower velocity layer and vice-versa. These time shifts are induced as a result of changes in fluid content or stress leading to compaction or extension in the reservoir or the overburden. Landrø and Stammeijer, 2004 define the relative change in elastic wave travel time due to changes in subsurface layer thicknesses (physical strain) and velocity as $\frac{\Delta t}{t} = \frac{\Delta z}{z} - \frac{\Delta v}{v}$, where $\frac{\Delta t}{t}$ is the relative time shift or time strain, $\frac{\Delta z}{z}$ is the vertical physical strain, and $\frac{\Delta v}{v}$ is the relative velocity change, which is a function of the lithology of the rock and the magnitude of the saturation change. For small physical strains, the time strain approximates to $\frac{\Delta t}{t} = -\frac{\Delta v}{v}$. Time shifts were extracted from full stacks of each of the four 3D monitor surveys relative to the baseline survey. MacBeth et al., 2020 provide a review of various methods of measurement of post-stack time-lapse time shifts. Dynamic time warping (DTW) algorithm with strain constraints as implemented by Hale, 2013 was used to extract the time shifts in this study. It is based on the minimization of the dissimilarity error between two traces: $e[i, q] = (f[i] - g[i + l])^2$, where i is the sample index, l is the integer lag or time shift between seismic traces, and f and g are the seismic amplitudes of the baseline and monitor traces, respectively.

The DTW implementation employed imposes constraints on the rate at which shifts may vary in time, i.e., a limit on maximum time strain, and this informs the choice of this algorithm. As relative velocity change can be approximated to the negative of time strain for small physical strains, we can derive from rock physics modelling the maximum saturation change (from available saturation logs), which is then used to model the maximum change in rock velocity. This provides constraints on the time strain. The rock physics modelling performed involved Gassmann (Gassmann, 1951) fluid substitution of brine with CO_2 following a patchy mixing (Brie et al., 1995). The mixing type was informed by field observations of velocity-saturation relationships for CO_2 storage in saline aquifers (Caspari et al., 2011). Fluid properties at in-situ conditions were computed using the FLAG fluid calculator (Han & Batzle, 2014). Constraints on time shifts and relative velocity change can also be derived from analogue datasets such as those published in MacBeth et al., 2019. These constraints are crucial for the accuracy of the results. Therefore, the atypical availability of the repeat CO_2 saturation logs in this dataset was essential to the successful application of this approach.

Results post-processing and noise removal

The obtained time strain volumes were afflicted by noise and artefacts. Most notably, speedup anomalies were observed directly beneath the slowdown anomalies. Such artefacts can result from data acquisition and processing, and from errors induced in the implementation of the time shift algorithms (MacBeth & Izadian, 2023). We removed speedup anomalies ($\frac{\Delta v}{v} > 0$) from the volumes as these are normally not expected when CO_2 replaces brine in a reservoir. Nevertheless, residual random noise was observed. These are attributed mainly to data acquisition challenges of source point co-location and varying ground conditions which may have introduced spurious time shifts in addition to amplitude anomalies throughout the volumes. A noise removal algorithm was developed to remove the residual noise from the time strain volumes. This relies on the availability of multiple monitor surveys. It tracks and preserves any features that are consistent across all the monitors, while discarding any non-consistent features. The design of this filter is based on an assumption that real plume anomalies would be consistent across the surveys while random noise would not. This is supported by the observed CO_2 plume distributions at well locations which remain largely the same over the injection period. Points of consistency in anomalies across all the monitors are identified as seed points, and the noise filter is applied, where the anomalies grow laterally and upwards starting from those seed points. This algorithm is based on the image segmentation algorithm of Flood Fill, and in this case effectively mimics the actual growth of the plume.

Data availability

The original dataset used in this study was made publicly available by the National Energy Technology Laboratory through the Energy Data eXchange, available at https://doi.org/10.18141/1854142.

References

Arts, R., Eiken, O., Chadwick, A., Zweigel, P., Van der Meer, L., & Zinszner, B. (2004). Monitoring of CO2 injected at Sleipner using time-lapse seismic data [Publisher: Elsevier]. *Energy*, *29*(9-10), 1383–1392.

Bauer, R., Will, R., Greenberg, S. E., & Whittaker, S. G. (2019). Illinois basin–Decatur project. In *Geophysics and geosequestration* (pp. 339–369). Cambridge University Press.

Benguigui, A., Roberts, G., & Shaw-Champion, M. (2012). Time-lapse 2D seismic steamflood monitoring-a case study from offshore republic of Congo, the Emeraude field. *74th EAGE Conference and Exhibition incorporating EUROPEC 2012*, cp–293.

Brie, A., Pampuri, F., Marsala, A., & Meazza, O. (1995). Shear sonic interpretation in gas-bearing sands. *SPE Annual Technical Conference and Exhibition?*, SPE–30595.

Caspari, E., Müller, T. M., & Gurevich, B. (2011). Time-lapse sonic logs reveal patchy CO2 saturation in-situ [_eprint: https://onlinelibrary.wiley.com/doi/pdf/10.1029/2011GL046959]. *Geophysical Research Letters*, *38*(13). https://doi.org/10.1029/2011GL046959

Cavanagh, A. J., & Haszeldine, S. (2014). The Sleipner storage site: Capillary flow modeling of a layered CO2 plume requires fractured shale barriers within the Utsira Formation [Publisher: Elsevier]. *International Journal of Greenhouse Gas Control*, *21*, 101–112.

Chadwick, R., Arts, R., & Eiken, O. (2005). 4D seismic quantification of a growing CO2 plume at Sleipner, North Sea [Issue: 1]. *Geological Society, London, Petroleum Geology Conference series*, *6*, 1385–1399.

Chadwick, R., Arts, R., Eiken, O., Kirby, G., Lindeberg, E., & Zweigel, P. (2004). 4D seismic imaging of an injected CO2 plume at the Sleipner Field, Central North Sea [Publisher: The Geological Society of London]. *Geological Society, London, Memoirs*, *29*(1), 311–320.

Couëslan, M. L., Ali, S., Campbell, A., Nutt, W., Leaney, W., Finley, R., & Greenberg, S. (2013). Monitoring CO2 injection for carbon capture and storage using time-lapse 3D VSPs [Publisher: Society of Exploration Geophysicists]. *The Leading Edge*, *32*(10), 1268–1276.

Couëslan, M. L., Butsch, R., Will, R., & Locke II, R. A. (2014). Integrated reservoir monitoring at the Illinois Basin–Decatur Project [Publisher: Elsevier]. *Energy Procedia*, *63*, 2836–2847.

Couëslan, M. L., Leetaru, H. E., Brice, T., Leaney, W. S., & McBride, J. H. (2009). Designing a seismic program for an industrial CCS site: Trials and tribulations [Publisher: Elsevier]. *Energy Procedia*, *1*(1), 2193–2200.

Dockrill, B., & Shipton, Z. K. (2010). Structural controls on leakage from a natural co2 geologic storage site: Central utah, usa. *Journal of Structural Geology*, *32*(11), 1768–1782.

Falahat, R., Shams, A., & MacBeth, C. (2011). Towards quantitative evaluation of gas injection using time-lapse seismic data [Publisher: European Association of Geoscientists & Engineers]. *Geophysical Prospecting*, *59*(2), 310–322.

Faulkner, D., Jackson, C., Lunn, R., Schlische, R., Shipton, Z., Wibberley, C., & Withjack, M. (2010). A review of recent developments concerning the structure, mechanics and fluid flow properties of fault zones. *Journal of Structural Geology*, *32*(11), 1557–1575.

Finley, R. J., Frailey, S. M., Leetaru, H. E., Senel, O., Couëslan, M. L., & Scott, M. (2013). Early operational experience at a one-million tonne CCS demonstration project, Decatur, Illinois, USA [Publisher: Elsevier]. *Energy Procedia*, *37*, 6149–6155.

Freiburg, J., Morse, D. G., Leetaru, H. E., Hoss, R. P., & Yan, Q. (2014). A depositional and diagenetic characterization of the Mt. Simon sandstone at the Illinois Basin-Decatur Project carbon capture and storage site, Decatur, Illinois, USA [Publisher: Illinois State Geological Survey, Prairie Research Institute, University of . . .].

Furre, A.-K., Eiken, O., Alnes, H., Vevatne, J. N., & Kiær, A. F. (2017). 20 years of monitoring CO2-injection at Sleipner [Publisher: Elsevier]. *Energy procedia*, *114*, 3916–3926.

Furre, A.-K., Kiær, A., & Eiken, O. (2015). CO2-induced seismic time shifts at Sleipner [Publisher: Society of Exploration Geophysicists and American Association of Petroleum ...]. *Interpretation*, *3*(3), SS23–SS35.

Gasda, S. E., Bachu, S., & Celia, M. A. (2004). Spatial characterization of the location of potentially leaky wells penetrating a deep saline aquifer in a mature sedimentary basin. *Environmental geology*, *46*, 707–720.

Gassmann, F. (1951). Über die elastizität poröser medien: Vierteljahrss-chrift der Naturforschenden Gesellschaft in Zurich, vol. 96.

Gilmore, K. A., Sahu, C. K., Benham, G. P., Neufeld, J. A., & Bickle, M. J. (2022). Leakage dynamics of fault zones: Experimental and analytical study with application to CO $_2$ storage. *Journal of Fluid Mechanics*, *931*, A31. https://doi.org/10.1017/jfm.2021.970

Grude, S., Landrø, M., & Osdal, B. (2013). Time-lapse pressure–saturation discrimination for CO2 storage at the Snøhvit field [Publisher: Elsevier]. *International Journal of Greenhouse Gas Control*, *19*, 369–378.

Hale, D. (2013). Dynamic warping of seismic images: Geophysics, 78. *S105–S115*.

Han, D., & Batzle, M. (2014). FLAG fluid calculator. *University of Houston Fluids/DHI Consortium*.

Hansen, O., Gilding, D., Nazarian, B., Osdal, B., Ringrose, P., Kristoffersen, J.-B., Eiken, O., & Hansen, H. (2013). Snøhvit: The history of injecting and storing 1 mt co2 in the fluvial tubåen fm. *Energy Procedia*, *37*, 3565–3573.

Ivandic, M., Juhlin, C., Lueth, S., Bergmann, P., Kashubin, A., Sopher, D., Ivanova, A., Baumann, G., & Henninges, J. (2015). Geophysical monitoring at the Ketzin pilot site for CO2 storage: New insights into the plume evolution [Publisher: Elsevier]. *International Journal of Greenhouse Gas Control*, *32*, 90–105.

Johnston, D. H. (2013). *Practical applications of time-lapse seismic data*. Society of Exploration Geophysicists.

Jung, N.-H., Han, W. S., Watson, Z., Graham, J. P., & Kim, K.-Y. (2014). Fault-controlled co2 leakage from natural reservoirs in the colorado plateau, east-central utah. *Earth and Planetary Science Letters*, *403*, 358–367.

Kang, M., Christian, S., Celia, M. A., Mauzerall, D. L., Bill, M., Miller, A. R., Chen, Y., Conrad, M. E., Darrah, T. H., & Jackson, R. B. (2016). Identification and characterization of high methane-emitting abandoned oil and gas wells. *Proceedings of the National Academy of Sciences*, *113*(48), 13636–13641.

Krevor, S., de Coninck, H., Gasda, S. E., Ghaleigh, N. S., de Gooyert, V., Hajibeygi, H., Juanes, R., Neufeld, J., Roberts, J. J., & Swennenhuis, F. (2023). Subsurface carbon dioxide and hydrogen storage for a sustainable energy future [Publisher: Nature Publishing Group UK London]. *Nature Reviews Earth & Environment*, 1–17.

Lahann, R., Rupp, J., Medina, C., Carlson, G., & Johnson, K. (2017). State of stress in the illinois basin and constraints on inducing failure. *Environmental Geosciences*, *24*(3), 123–150.

Landrø, M., & Stammeijer, J. (2004). Quantitative estimation of compaction and velocity changes using 4D impedance and traveltime changes [Publisher: Society of Exploration Geophysicists]. *Geophysics*, *69*(4), 949–957.

Leetaru, H., & Freiburg, J. T. (2014). Litho-facies and reservoir characterization of the Mt Simon Sandstone at the Illinois Basin–Decatur Project [Publisher: Wiley Online Library]. *Greenhouse Gases: Science and Technology*, *4*(5), 580–595.

MacBeth, C., Amini, H., & Izadian, S. (2020). Methods of measurement for 4D seismic post-stack time shifts [Publisher: Wiley Online Library]. *Geophysical Prospecting*, *68*(9), 2637–2664.

MacBeth, C., Mangriotis, M.-D., & Amini, H. (2019). Post-stack 4D seismic time-shifts: Interpretation and evaluation [Publisher: European Association of Geoscientists & Engineers]. *Geophysical Prospecting*, *67*(1), 3–31.

MacBeth, C., & Izadian, S. (2023). A review and analysis of errors in post-stack time-shift interpretation [Publisher: European Association of Geoscientists & Engineers]. *Geophysical Prospecting*, *71*(8), 1497–1522.

Miocic, J. M., Gilfillan, S. M., Roberts, J. J., Edlmann, K., McDermott, C. I., & Haszeldine, R. S. (2016). Controls on co2 storage security in natural reservoirs and implications for co2 storage site selection. *International Journal of Greenhouse Gas Control*, *51*, 118–125.

Nordbotten, J. M., Kavetski, D., Celia, M. A., & Bachu, S. (2009). Model for co2 leakage including multiple geological layers and multiple leaky wells. *Environmental science & technology*, *43*(3), 743–749.

Onishi, T., Nguyen, M. C., Carey, J. W., Will, B., Zaluski, W., Bowen, D. W., Devault, B. C., Duguid, A., Zhou, Q., Fairweather, S. H., et al. (2019). Potential co2 and brine leakage through wellbore pathways for geologic co2 sequestration using the national risk assessment partnership tools: Application to the big sky regional partnership. *International Journal of Greenhouse Gas Control*, *81*, 44–65.

Pörtner, H., Roberts, D. C., Poloczanska, E., Mintenbeck, K., Tignor, M., Alegría, A., Craig, M., Langsdorf, S., Löschke, S., Möller, V., et al. (2022). IPCC, 2022: Summary for policymakers [Publisher: Cambridge University Pres].

Ringrose, P., Andrews, J., Zweigel, P., Furre, A.-K., Hern, B., & Nazarian, B. (2022). Why ccs is not like reverse gas engineering. *First Break*, *40*(10), 85–91.

Roach, L. A., & White, D. (2018). Evolution of a deep co2 plume from time-lapse seismic imaging at the aquistore storage site, saskatchewan, canada. *International Journal of Greenhouse Gas Control*, *74*, 79–86.

Santos, J. M., Davolio, A., MacBeth, C., & Schiozer, D. J. (2016). 4D seismic interpretation of the Norne Field-a semi-quantitative approach [Issue: 1]. *78th EAGE Conference and Exhibition 2016*, *2016*, 1–5.

Stork, C. (2020). How does the thin near surface of the earth produce 10–100 times more noise on land seismic data than on marine data? *First Break*, *38*(8), 67–75.

Strandli, C. W., & Benson, S. M. (2013). Identifying diagnostics for reservoir structure and co2 plume migration from multilevel pressure measurements. *Water Resources Research*, *49*(6), 3462–3475.

Strandli, C. W., Mehnert, E., & Benson, S. M. (2014). Co2 plume tracking and history matching using multilevel pressure monitoring at the illinois basin–decatur project. *Energy Procedia*, *63*, 4473–4484.

Swager, L. (2019). *ADM CCS1 Injection Well Mechanical Integrity Report March 2019 Pulsed Neutron eXtreme* (tech. rep.).

Yang, Z., Xu, T., Wang, F., Yang, Y., Li, X., & Zhao, N. (2018). Impact of inner reservoir faults on migration and storage of injected co2. *International Journal of Greenhouse Gas Control*, *72*, 14–25.

Zaluski, W., & Lee, S.-Y. (2021). *2020 IBDP Final Static Geological Model Development and Dynamic Modelling* (tech. rep.).

Zhang, L., Yang, Q., Zhang, S., Shan, L., Jiang, Q., & Sun, M. (2024). Enhanced co2 storage efficiency due to the impact of faults on co2 migration in an interbedded saline aquifer. *International Journal of Greenhouse Gas Control*, *133*, 104104.

Acknowledgments. The authors wish to acknowledge support from SLB and Ikon Science for academic licenses for Petrel and RokDoc. We thank the Petroleum Technology Development Fund for providing the funding for this research.

Supplementary Information.

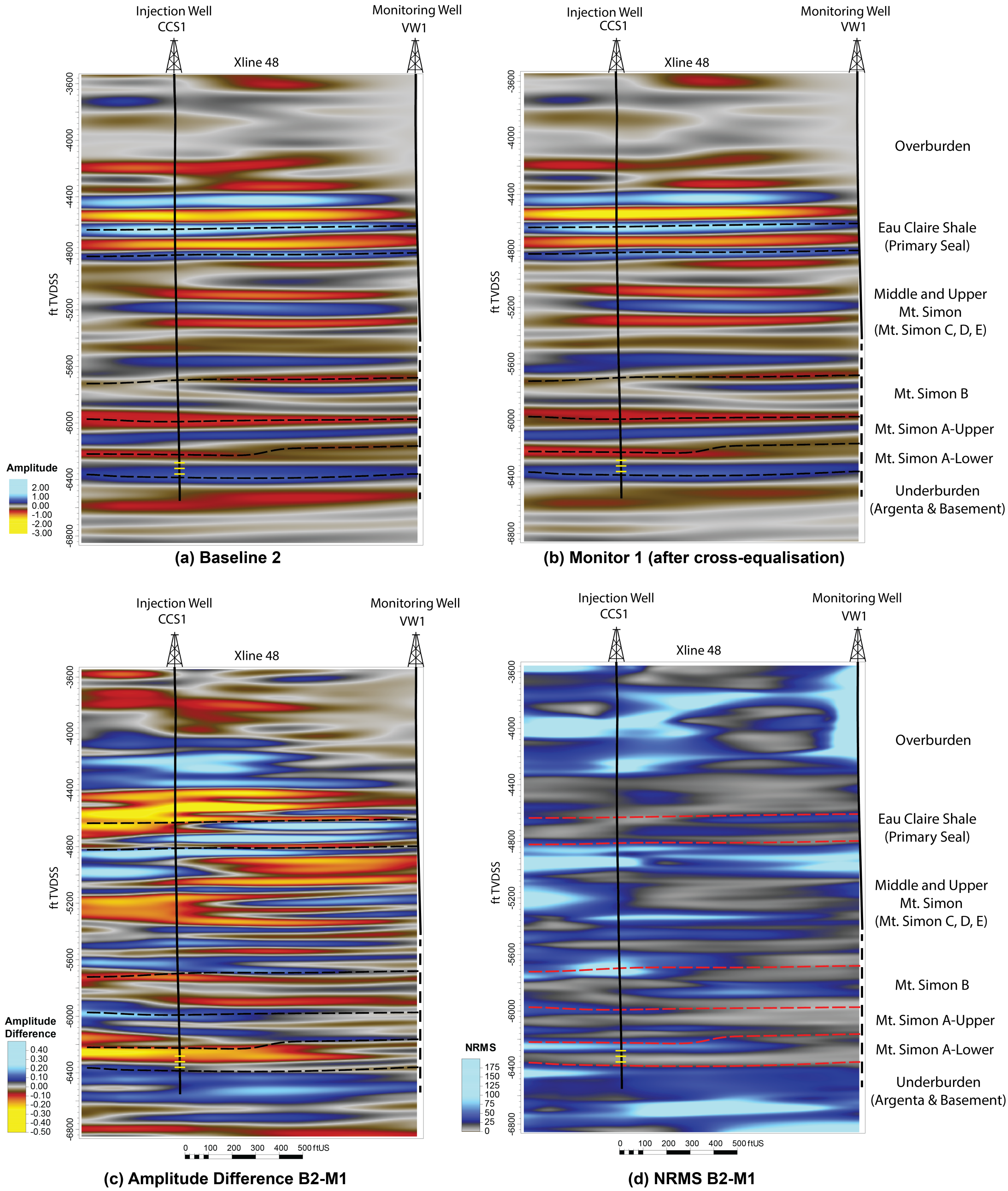

Fig. S.1 Cross-sectional views of (a) Baseline 2 amplitudes, (b) Monitor 1 amplitudes after cross-equalisation, (c) Amplitude difference, and (d) NRMS.

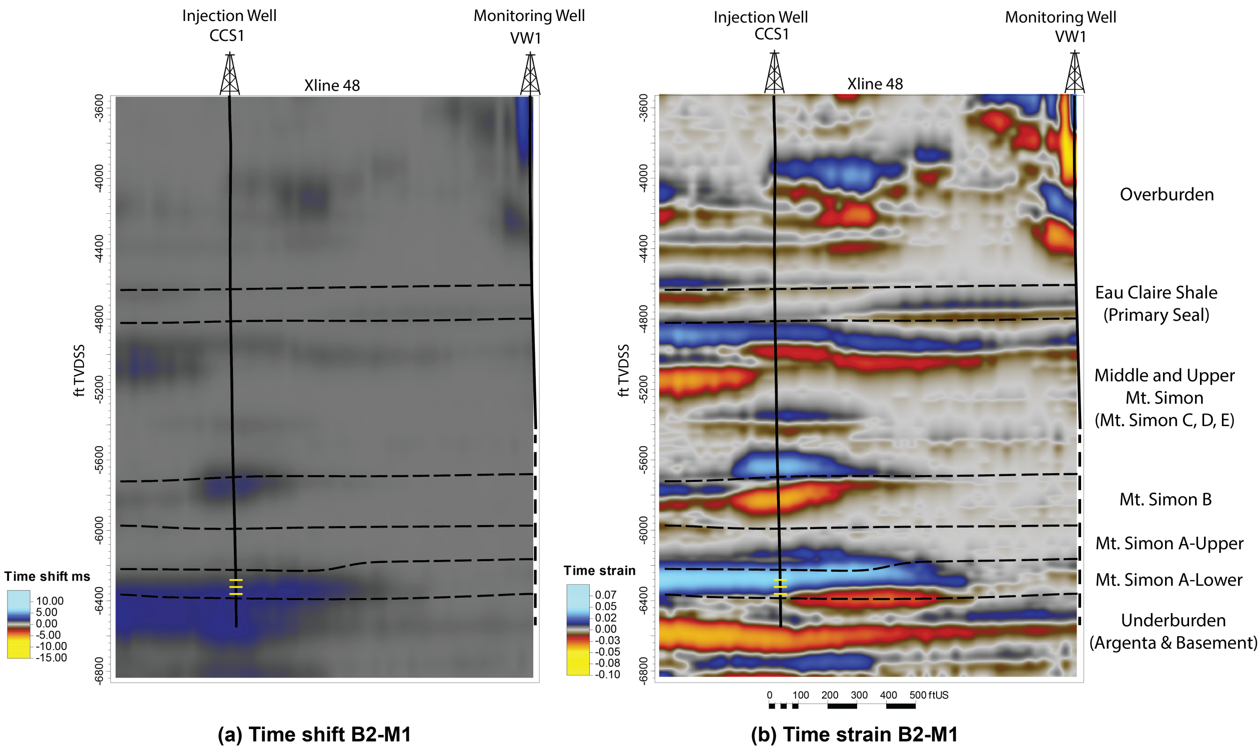

Fig. S.2 Cross-sectional views of time shift and time strain (first derivative of time shift) between Baseline 2 and Monitor 1. The image is clearer than amplitude difference and NRMS attributes.

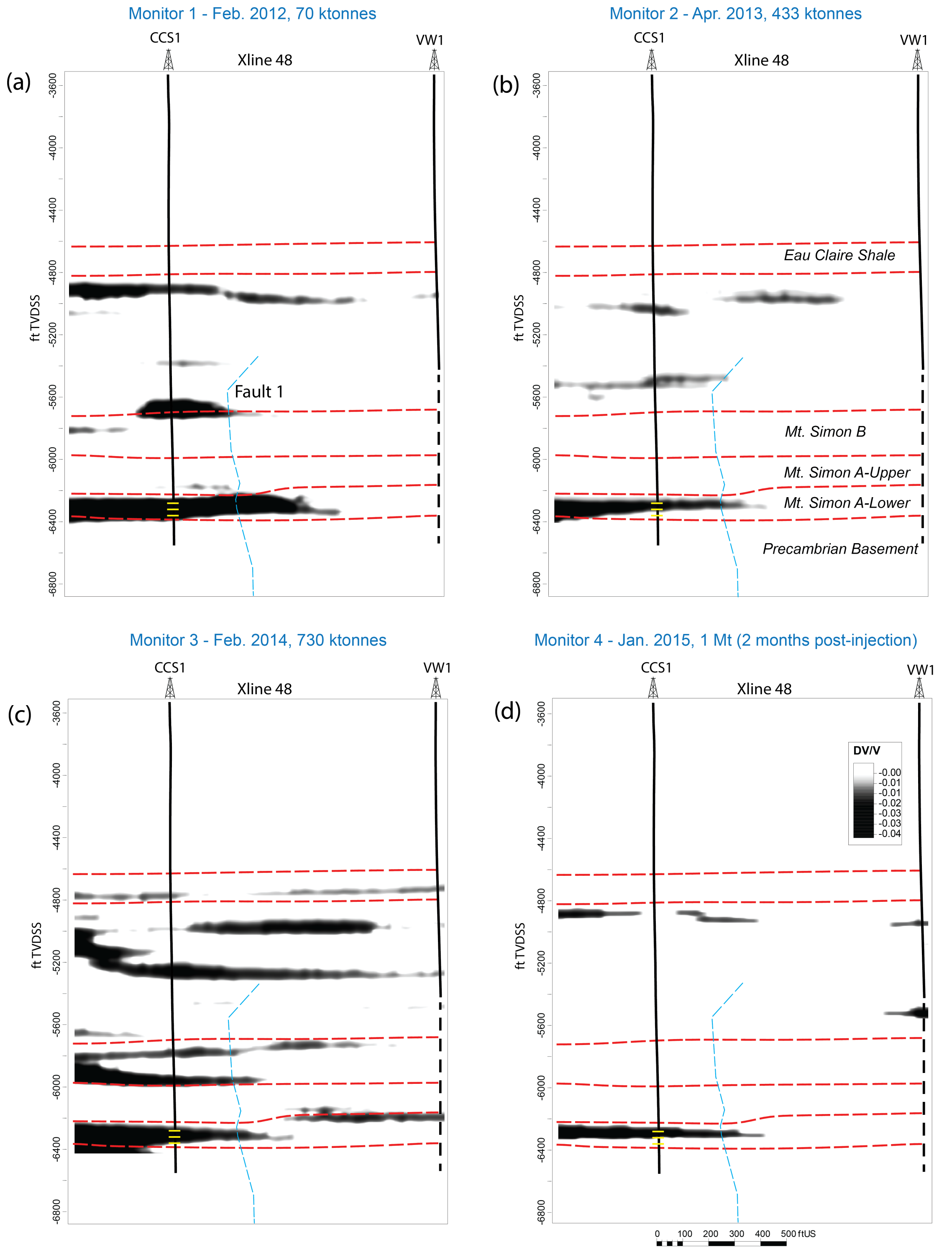

Fig. S.3 Cross-sectional views of interpreted plume layers for all four monitors referenced to the baseline. The plume features are qualitatively very similar as observed within the narrow monitoring cubes.